Published in final edited form as:
J Pharm Sci. 2010 February ; 99(2): 730–740. doi:10.1002/jps.21863.

Hydration Effects on Skin Microstructure as Probed by High-Resolution Cryo-Scanning Electron Microscopy and Mechanistic Implications to Enhanced Transcutaneous Delivery of Biomacromolecules

Grace Tan[1], **Peng Xu**[1], **Louise B. Lawson**[2], **Jibao He**[3], **Lucia C. Freytag**[2], **John D. Clements**[2], and **Vijay T. John**[1]

[1]Department of Chemical & Biomolecular Engineering, Tulane University, New Orleans, Louisiana 70118

[2]Department of Microbiology & Immunology, Tulane University School of Medicine, New Orleans, Louisiana 70112

[3]Coordinated Instrumentation Facility, Tulane University, New Orleans, Louisiana 70118

Abstract

Although hydration is long known to improve the permeability of skin, penetration of macromolecules such as proteins is limited and the understanding of enhanced transport is based on empirical observations. This study uses high-resolution cryo-scanning electron microscopy to visualize microstructural changes in the stratum corneum (SC) and enable a mechanistic interpretation of biomacromolecule penetration through highly hydrated porcine skin. Swollen corneocytes, separation of lipid bilayers in the SC intercellular space to form cisternae, and networks of spherical particulates are observed in porcine skin tissue hydrated for a period of 4–10 h. This is explained through compaction of skin lipids when hydrated, a reversal in the conformational transition from unilamellar liposomes in lamellar granules to lamellae between keratinocytes when the SC skin barrier is initially established. Confocal microscopy studies show distinct enhancement in penetration of fluorescein isothiocyanate-bovine serum albumin (FITC-BSA) through skin hydrated for 4–10 h, and limited penetration of FITC-BSA once skin is restored to its natively hydrated structure when exposed to the environment for 2–3 h. These results demonstrate the effectiveness of a 4–10 h hydration period to enhance transcutaneous penetration of large biomacromolecules without permanently damaging the skin.

Keywords

transdermal; lipids; imaging methods; hydration; vaccine delivery; cryo-SEM; confocal laser scanning microscopy; skin; transcutaneous; ceramides

INTRODUCTION

A number of studies have been conducted on the skin, in particular the stratum corneum (SC), which functions as the main barrier to the human body.[1–6] Its role is to regulate transepidermal

Correspondence to: Vijay T. John (Telephone: 1-504-865-5883; Fax: 1-504-865-6744; vijay.john@tulane.edu).

water loss and restrict the entry of foreign bodies and pathogens. Commercially available products utilizing transdermal delivery have been mainly limited to low molecular weight lipophilic drugs (MW < 500 Da)7, with larger molecules (MW > 500 Da) facing penetration difficulties. From the perspective of immunology8¯11 and drug delivery,11›12 the penetration of macromolecular compounds through the skin is of much interest.

Needle-free transcutaneous immunization is of potential advantage in avoiding needle-borne disease associated with improper disposal and needle reuse,[13] and offers increased patient compliance. It has also been shown to promote mucosal as well as systemic antibody responses, which is beneficial in protection against infectious agents entering through the oral, nasal, or other mucosal surface. The efficacy of transcutaneous immunization has been shown in several animal models in which significant immune response and, in some cases, protection from exposure to pathogens was demonstrated.[14–17] Clinical trials have also indicated the safety and efficacy of this administration route in humans.[18–20] Such needle-free immunization targets the vast network of antigen presenting cells in the dermis and epidermis.[21] The antigen only needs to penetrate through the SC to reach the antigen presenting cells, known as Langerhans cells, which upon activation following phagocytosis of the antigen, migrate out of the skin into the draining lymph node, present the antigen to T cells, and subsequently elicit an immune response.[22] However, due to the impervious nature of the SC towards macromolecules, a suitable penetration enhancer should substantially improve transport of macromolecules through the skin. A variety of technologies have been developed to enhance penetration for macromolecules through the skin, including the use of microneedles,[23–25] electroporation,[26,27] laser generated pressure waves,[28–31] hyperthermia,[32] low-frequency sonophoresis,[33–39] iontophoresis,[40–43] penetration enhancers,[44–51] or a combination of these methods.[52–54] Many penetration enhancement techniques face inherent challenges, such as scale-up and safety concerns.[7]

Water is the most natural and biocompatible penetration enhancer known to improve the permeability of skin.[22,55–58] Changes to the SC have been monitored using a variety of techniques including freeze-fracture electron microscopy and neutron scattering. Earlier work on hydration appeared to indicate negligible changes in SC ultrastructure.[59,60] However, in the more recent literature there appears to be increasing evidence that extensive hydration using occlusion methods may lead to disruptions of the lipid ultrastructure.[2,3,61–63] The use of water-based formulations for transcutaneous delivery of vaccines have provided encouraging results.[18] However, there is a lack of articles in the literature relating both the changes in skin microstructure with hydration and the penetration of macromolecules through hydrated skin.

In this article, we focus on the use of cryo-scanning electron microscopy (cryo-SEM) to explore how extensive hydration changes the SC to allow the penetration of macromolecules. We clearly show that the SC is a dynamic structure, where extended hydration (>8 h) swells corneocytes, creates intercorneocyte ruptures, and causes microstructural changes in lipid self-assembly. The implications to biomacromolecule penetration are significant, since these disruptions allow penetration through the barrier of the SC. The disruptions are reversible, as removing the hydration source easily restores the barrier. Through high-resolution cryo-SEM, we are able to understand microstructural changes in the SC as a function of hydration, and are able to image ultrastructural changes in lipid self-assembly. We propose a qualitative model to understand how corneocyte swelling with hydration leads to perturbations in intercorneocyte lipid conformations and allows the generation of new pathways for water penetration.

MATERIALS AND METHODS

Materials

Fluorescein isothiocyanate-bovine serum albumin (FITC-BSA) was purchased from Sigma–Aldrich (St. Louis, MO). Distilled water was used to hydrate porcine skin. 0.1M phosphate buffer solution (pH 7.4) containing 50mg/mL FITC-BSA was prepared and stored at 4°C.

Preparation of Porcine Skin Tissue

Full-thickness porcine skin from newborn to 1-month-old pigs, provided by the Louisiana State University AgCenter Swine Unit, was immersed in liquid nitrogen to rapidly freeze the tissue and stored in the freezer. For experimentation, a piece of frozen porcine skin was thawed at room temperature. The hair was trimmed down to ~1–2mm and the subcutaneous fat was removed.

Hydration of Porcine Skin Using an Occlusive Wet Hydration Patch

The gauze portion of an adhesive bandage or “Band-aid” was fully wetted with distilled water before placing the patch onto the surface of porcine skin. The porcine skin, partially occluded by the patch, was enclosed in a petri dish such that the skin surface not exposed to water would not dehydrate with time (Fig. 1). (Note: Enclosure of porcine skin in a petri dish was chosen because regions of porcine skin not exposed to water from the bandage will become dry within an hour if conducted in an open system). After 4–10 h of hydration, the patch was discarded and the skin was immediately plunged in liquid nitrogen prior to sectioning of the sample for cryo-SEM.

Cryo-Scanning Electron Microscopy

Porcine skin frozen in liquid nitrogen was sectioned to obtain a thin slice of ~1mm thickness. The strip of pigskin was mounted vertically on the cryo-SEM sample holder with a small amount of Tissue-Tek adhesive (Sakura, Ted Pella, Redding, PA). The sample was rapidly plunged into liquid nitrogen slushed lower than −190°C (Gatan, Pleasanton, CA, Alto 2500), withdrawn into a vacuum transfer device under the protection of high vacuum, and transferred into the cryo-preparation chamber where the temperature was maintained at −130°C and the anticontaminator at around −188°C. The porcine skin tissue was freeze fractured using the flat edge of a cold knife maintained at −130°C and sublimated for 5min at −95°C to etch away surface water and expose the internal structural features. After sublimation, the temperature of the stage was adjusted back to −130°C and the sample was sputter coated with platinum at 10 mA for 85 s. The sample was then transferred into the main chamber of the Field Emission SEM (Hitachi S-4800) via an interlocked airlock and mounted onto a cold stage module (−130° C) fitted to the SEM stage. Images were acquired at a voltage of 3 kV and at a working distance of ~6mm.

Loading of FITC-BSA on Skin Tissue

A 20-μL droplet of FITC-BSA (50 mg/mL) was deposited at the center of the skin tissue to prevent spilling of the protein solution down the sides of the specimen. The porcine skin was kept covered in a petri dish so that both the fluorescent protein and the skin tissue would not dry out. Aluminum foil was wrapped around the petri dish to prevent photo-bleaching of the fluorescent protein. One hour after loading of the fluorescent protein, excess FITC-BSA was wiped off the skin surface. The skin surface was rinsed with water and pat dry with a kimwipe. Fixation of the skin samples was carried out by first soaking the samples in a 4% paraformaldehyde solution prepared in 1 × PBS and subsequently in a series of sucrose solutions (20%, 30%, and 40% sucrose). The samples were then embedded in Tissue-Tek and kept frozen at −80°C prior to cutting 8 μm thick cross-sections of the samples using a cryostat

(Micron HM505E). The Tissue-Tek surrounding the skin sections on the glass slides was removed by immersing the glass slides in 1× PBS buffer for 3–5 min, following which the glass slides were wiped dry and the skin sections were mounted in Prolong Gold antifade reagent (Invitrogen, Carlsbad, CA) containing 4′,6-diamidino-2-phenylindole (DAPI). This step enables staining of the cell nuclei with DAPI and makes the fluorescent compounds more resistant to photo-bleaching.

Confocal Microscopy

A confocal microscope (Leica DMIRE2) was used to image the cross-sections of porcine skin tissue. The system is equipped with an argon and diode laser. Two different tracks were used to monitor FITC-BSA and the DAPI-stained cell nuclei in skin tissue independently. FITC-BSA was excited at 488 nm and the fluorescent emission signals are represented by a green color. The DAPI-stained cell nuclei were excited by the diode laser at 405 nm and are shown by a blue color. The stained cell nuclei help identify structural features and determining the orientation of the skin tissue in the images. Images were acquired using a 20× objective lens. The pinhole was adjusted to 72.76 μm and an average of eight scans was collected for each image.

RESULTS AND DISCUSSION

In vitro experiments were conducted on porcine skin because the SC lipid composition in porcine skin bears the closest resemblance to human skin lipids compared to other animals such as the mouse, sheep, or cow.[64] The porcine SC is slightly thicker than in humans; however, the thickness of the entire epidermis is very similar between the two species. The lipid composition and total lipid content of the SC is quite similar as well.[65] Furthermore, a number of permeation studies conducted either *in vivo* or *in vitro* show permeability resemblance in human and porcine skin.[66–69] Specifically, skin from weanling pigs most closely approximates the permeation resistance of human forearm skin;[64] for this reason, skin from animals 1 month of age or younger was used. For imaging purposes, cryo-SEM is a suitable tool to visualize skin tissue immobilized in the frozen state in three-dimensional form.[70] It is preferred over conventional SEM due to omission of artifacts induced in fixing and dehydration procedures, and provides a faithful representation of water-swollen structures. Since water plays an important role in lipid self-assembly, it is important to avoid dehydration procedures to preserve native lipid microstructures. Cryo-SEM enables easy comparison of overall ultrastructural changes throughout the skin tissue and provides clear visualization of depth profiles. Moreover, the ability to etch water from the skin tissue allows determination of changes in corneocyte keratin density, and improves visualization of intercellular separations. Our study is based on results that have been repeated at least three times, with a total of 121 cryo-SEM images and 81 confocal microscopy images taken.

Untreated Porcine Skin

Native, untreated porcine skin tissue was first imaged on the cryo-SEM as control, and as a reliable comparison for highly hydrated skin tissue. A small piece of skin sample was thawed at room temperature and immediately imaged. The porcine skin samples were cryo-fractured to reveal a clean cross-section of the skin tissue and coated with a thin layer of platinum to prevent sample charging during imaging. Figure 2 and Figure 3 show typical views of native, untreated porcine skin at low and high magnification, respectively. The SC of untreated porcine skin (Fig. 2) consists of tightly apposed corneocytes with minimal intercellular space. The thickness of the SC is slightly more than 10 μm and consists of 27–30 corneocyte layers. In the deeper layers of the SC, the corneocytes assume a more irregular shape, with thicker regions ~700–1000nm (Fig. 3b). More than two-thirds of the SC (~20 corneocyte layers), located closer to the skin surface, consist of 150–300nm thick flat corneocyte cells (Fig. 3c). More corneocyte

layers in porcine skin are observed here than that reported for human skin, which is between 12–20 layers.[2] It should be noted that pig SC is typically thicker than human SC.[65] Since porcine SC thickens much faster with maturity compared to human SC,[65] new-born to 1-month-old pigskin was used to reduce the disparity between the two species.

Hydration of Porcine Skin Using an Occlusive Wet Hydration Patch

In order to compare natively hydrated porcine skin with externally hydrated skin, we hydrated porcine skin tissue using a wet hydration patch. This is a simple hydration procedure where the gauze part of an adhesive bandage or "Band-aid" was periodically wetted with water and attached onto the porcine skin surface. The skin tissue with the wet patch affixed was placed on the microscope slide and kept enclosed in a petri dish containing a little water during the entire duration of hydration to ensure that parts of the skin tissue not covered by the patch did not dry out, and stayed natively hydrated. After the intended duration of water exposure to the gauze-covered region of the skin, the hydrated skin tissue was immediately frozen in liquid nitrogen and imaged on the cryo-SEM.

External hydration of porcine skin for an hour does not result in any significant changes as shown in Figure 4a, where it is clearly observed that the SC still consists of tightly packed corneocyte layers. Figure 4b shows the cross-section of skin tissue hydrated for 6 h and indicates a threefold increase in the thickness of the SC. Due to the variability in skin tissue from different animals, such gross changes in the SC are seen for time periods ranging from 4 to 10 h of hydration using the occlusion patch. In all samples, we observe that at least several locations in the SC lose their compact corneocyte structure and expand three- to fourfold to a thickness of 30– 40 μm. Separation of the lamellar lipids between corneocytes to form small cisternae is observed in multiple locations throughout the SC, and is especially evident in the middle layers (Fig. 4b). The separation of lipid bilayers in highly hydrated skin shows that the intercorneocyte lipid region has been compromised. The inset to Figure 4b clearly reveals that the keratin-filled corneocyte cells, which can bind substantial amounts of water have become swollen. With slight etching, unbound water in the cross-section of corneocytes is removed, clearly revealing a distinct keratin filament pattern and a more porous internal corneocyte composition. The results presented above show that significant alterations can be inflicted upon the SC when hydrated sufficiently.

We have carried out time dependent studies on the change to the SC when subjected to hydration, and the results are summarized through Figure 5 illustrating the SC thickness as a function of time. The data plotted with the standard deviation shown is for multiple points taken from the skin of one animal. There appears to be three rough stages of hydration. In Stage 1 which extends for around 2 h, there is a small expansion of the SC with about a 10–20% increase in thickness from around 8mm to around 9mm. With increasing hydration time, there is further swelling of the SC and small spacings between corneocytes are observed which leads to the apparent increase in thickness to 12–14 mm. (Stage II). When hydration is extensive, ruptures are observed with a three- to fourfold expansion of the SC (Stage III). The data point in Stage III has a comparatively larger standard deviation. This is because the standard deviation accounts for the thickness of the ruptured sections of the SC as well as that of nonruptured sections. The corresponding cryo-electron microscopy images of the unruptured and ruptured sections (Stage III) are shown in Figure 6. Although Figure 5 shows the general trend for porcine skin when hydrated, the ruptures may occur at an earlier or later time due to variability of skin tissue from different animals. This explains the slight overlap in the hydration time range for Stage II and Stage III. In fact, we have observed ruptures occurring in skin tissue that was hydrated for as short as 4 h.

Spherical/Vesicular Lipid Structures in Cisternae

Figure 7a shows the interiors of two cisternae containing particulate matter in highly hydrated porcine skin. Contents of cisternae consist of individual or agglomerated polydispersed spheres (or beads) strung on filamentous material as shown in the high-resolution micrographs of Figure 7b and c. These features are not artifacts and have been observed in all extensively hydrated porcine skin samples that we have examined. They have also been observed (but in much lower resolution) in extensively hydrated human skin samples.[62]

Since these cisternae represent ruptured intercorneocyte regions, the spherical entities probably represent skin lipids (originally existing in the lipid bilayers) that have undergone a conformational change. These empirical observations obtained through high-resolution cryo-electron microscopy, helped us determine a mechanism for the formation of cisternae and the phase-segregated structures within the cisternae, which is illustrated through Figure 8. As the corneocytes swell due to the affinity of keratin filaments for water, bending stresses arise at the corneocyte edges where the curvatures are the highest, with the approximate analogy of long flat pancake-like structures swelling to long prolate ellipsoidal structures, with the highest curvatures at the ends of the major axis. These stresses lead to ruptures in the extracellular lipid matrix and allow water penetration. The resultant change in the lipid–water phase composition may lead to modifications in the lipid conformations with the beadlike assemblies in Figure 7b and c occurring due to phase segregation between the water insoluble lipids and water. We have observed such conformation changes in other extended lipid systems where crystalline mesophases of tubular hexagonal arrays roll up into multilamellar vesicles upon water addition.[71] Thus, we propose that water intrusion through the ruptured path-ways leads to phase segregation of the water insoluble ceramide lipids in skin and the beaded structures. We do not know what the filamentous material is, whether they represent tubule-like lipid structures or fragments of corneodesmosomes. After the ruptures take place, we also see a small compression (or a less swollen state) in the corneocytes adjacent to the rupture.

Penetration Studies of Fluorescein Isothiocyanate-Bovine Serum Albumin (FITC-BSA) in Control Versus Highly Hydrated Skin

In order to determine whether hydration has sufficiently opened up pathways for penetration of large molecules, we compared the penetration of a fluorescent-labeled model protein (FITC-BSA) through both natively hydrated and extensively hydrated skin (8 h hydration) using confocal microscopy. The FITC-BSA solution was loaded on top of the skin tissue for an hour in an environmental chamber under conditions that prevented dehydration and photo-bleaching of the fluorescent probe. To allow for an even comparison between natively hydrated and highly hydrated samples, the same amount of fluorescent protein and identical imaging conditions were used in all cases. The green color in Figure 9 indicates the collective emission signal of the fluorescent protein in the skin tissue while the blue color shows DAPI-stained nuclei of cells. Very limited movement of FITC-BSA through native porcine skin was observed, with FITC-BSA simply accumulating on the skin surface (Fig. 9a). In contrast, Figure 9b clearly shows significantly enhanced penetration of the fluorescent protein through highly hydrated skin with penetration deep into the dermis. There is a general widespread distribution of the protein throughout the skin tissue instead of distinct focused spots of penetration, signifying that the transport pathways of the protein are diffused throughout the skin.

Recovery of Skin Ultrastructure

To test the reversibility of porcine skin hydrated for 4–10 h, the wet patch was removed to let the skin recover at ambient conditions for 2–3 h, before imaging the skin tissue on the cryo-SEM. Figure 10 shows the cryo-SEM of restored porcine skin. We observe that the corneocytes resume a compact packing and the ruptures have disappeared. Dilations and cisternae are not noticed after skin recovery. The observation also lends credibility to the hypothesis that skin

lipid conformations are based on compositions in the lipid–water phase diagram. As the water content in the SC returns to the natively hydrated levels, the intercorneocyte lipids again form extended structures. To further test the barrier properties of the recovered SC, we carried out the FITC-BSA penetration experiment. Figure 9c indicates restoration of the penetration barrier. We anticipate the ability of the skin to recover to be more potent in live subjects. This may be an advantage of hydration over skin abrasion in penetration technologies, since skin restoration after abrasion is based on a much longer skin turnover time period.

In summary, high-resolution cryo-SEM results demonstrate that a sufficient hydration time is required before gross changes occur in the SC ultrastructure, which can be correlated to an enhancement in protein penetration. Since neither erythema nor complications of dermatitis have been reported for a 6–24 h exposure to water,[62,72–75] we believe that this approach would help to overcome the skin barrier safely and reversibly. The results presented in this study have to be viewed with caution when translated to human subjects. We must realize that we are using an *in vitro* procedure with porcine skin and a model protein. While depth of penetration can be seen through confocal microscopy, it is hard to quantify the level of penetration. Occlusive vaccine patch technology studies on human subjects with hydration do show a degree of efficacy.[18] But these are empirical studies that do not correlate penetration to skin ultrastructure. We believe that this work offers an explanation of why occlusive patch technology is feasible especially when the skin is extensively hydrated. It is important to keep the SC continuously hydrated under an occlusive patch for extended periods to create such disruptions. From a technological perspective, our results clearly indicate the viability of using a “wet patch” to facilitate vaccine antigen penetration through the SC and presentation to the underlying dendritic cells of the immune system. On an alternate note, the ability of extended hydration to dramatically change SC structure calls for careful interpretation of skin penetration experiments conducted in diffusion cells. Hydration of the SC side of the skin for extended periods to equilibrate the skin prior to penetration studies would have altered the SC permeability significantly. An improvement in penetration is also expected when water-based formulations are applied on the skin for an extended period of time since the skin would have been hydrated sufficiently for new penetration pathways to emerge.

Acknowledgments

Support from the National Institutes of Health (grant 1RO1EB006493–01) is gratefully acknowledged. L. B. L. was a recipient of a Ruth L. Kirschstein National Research Service Award (F32-AI066682) from the National Institutes of Health.

REFERENCES

1. Chen YL, Wiedmann TS. Human stratum corneum lipids have a distorted orthorhombic packing at the surface of cohesive failure. J Invest Dermatol 1996;107:15–19. [PubMed: 8752832]
2. Bouwstra JA, de Graaff A, Gooris GS, Nijsse J, Wiechers JW, van Aelst AC. Water distribution and related morphology in human stratum corneum at different hydration levels. J Invest Dermatol 2003;120:750–758. [PubMed: 12713576]
3. Charalambopoulou GC, Steroptos TA, Hauss T, Stubos AK, Kanellopoulos NK. Structural alterations of fully hydrated human stratum corneum. Phys B 2004;350:e603–e606.
4. Pieper JGC, Steriotis T, Vasenkov S, Desmedt A, Lechner RE. Water diffusion in fully hydrated porcine stratum corneum. Chem Phys 2003;292:465–476.
5. Rawlings AV, Scott IR, Harding CR, Bowser PA. Stratum corneum moisturization at the molecular level. J Invest Dermatol 1994;103:731–741. [PubMed: 7963664]
6. Rawlings AV, Matts PJ. Stratum corneum moisturization at the molecular level: An update in relation to the dry skin cycle. J Invest Dermatol 2005;124:1099–1110. [PubMed: 15955083]
7. Mitragotri S. Breaking the skin barrier. Adv Drug Deliv Rev 2004;56:555–556. [PubMed: 15019744]
8. Mitragotri S. Immunization without needles. Nat Rev Immunol 2005;5:905–916. [PubMed: 16239901]

9. Giudice EL, Campbell JD. Needle-free vaccine delivery. Adv Drug Deliv Rev 2006;58:68–89. [PubMed: 16564111]
10. O'Hagan DT, Rappuoli R. Novel approaches to vaccine delivery. Pharm Res 2004;21:1519–1530. [PubMed: 15497674]
11. Pillai O, Nair V, Jain AK, Thomas NS, Panchagnula R. Noninvasive transdermal delivery of peptides and proteins. Drugs Future 2001;26:779–791.
12. Prausnitz MR, Mitragotri S, Langer R. Current status and future potential of transdermal drug delivery. Nat Rev 2004;3:115–124.
13. Yu RC, Abrams DC, Alaibac M, Chu AC. Morphological and quantitative analyses of normal epidermal Langerhans cells using confocal scanning laser microscopy. Br J Dermatol 1994;131:843–848. [PubMed: 7857837]
14. Kenney RT, Yu J, Guebre-Xabier M, Frech SA, Lambert A, Heller BA, Ellingsworth LR, Eyles JE, Williamson ED, Glenn GM. Induction of protective immunity against lethal anthrax challenge with a patch. J Infect Dis 2004;190:774–782. [PubMed: 15272406]
15. Glynn A, Freytag LC, Clements JD. Effect of homologous and heterologous prime-boost on the immune response to recombinant plague antigens. Vaccine 2005;23:1957–1965. [PubMed: 15734068]
16. Glynn A, Roy CJ, Powell BS, Jeffrey J, Adamovicz JJ, Freytag LC, Clements JD. Protection against aerosolized Yersinia pestis challenge following homologous and heterologous prime-boost with recombinant plague antigens. Infect Immun 2005;73:5256–5261. [PubMed: 16041052]
17. Peachman KK, Rao M, Alving CR, Burge R, Leppla SH, Rao VB, Matyas GR. Correlation between lethal toxin-neutralizing antibody titers and protection from intranasal challenge with Bacillus anthracis Ames strain spores in mice after transcutaneous immunization with recombinant anthrax protective antigen. Infect Immun 2006;74:794–797. [PubMed: 16369043]
18. Glenn GM, Taylor DN, Li X, Frankel S, Montemarano A, Alving CR. Transcutaneous immunization: A human vaccine delivery strategy using a patch. Nat Med 2000;6:1403–1406. [PubMed: 11100128]
19. Frerichs DM, Ellingsworth LR, Frech SA, Flyer DC, Villar CP, Yu J, Glenn GM. Controlled, single-step, stratum corneum disruption as a pretreatment for immunization via a patch. Vaccine 2008;26:2782–2787. [PubMed: 18455283]
20. Glenn GM, Kenney RT, Hammond SA, Ellings-worth LR. Transcutaneous immunization and immunostimulant strategies. Immunol Allergy Clin North America 2003;23:787–813.
21. Tuting T, Storkus WJ, Falo LD Jr. DNA immunization targeting the skin: Molecular control of adaptive immunity. J Invest Dermatol 1998;111:183–188. [PubMed: 9699714]
22. Glenn GM, Scharton-Kersten T, Alving CR. Advances in vaccine delivery: Transcutaneous immunisation. Exp Opin Invest Drugs 1999;8:797–805.
23. Henry S, McAllister DV, Allen MG, Prausnitz MR. Microfabricated microneedles: A novel approach to transdermal drug delivery. J Pharm Sci 1998;87:922–925. [PubMed: 9687334]
24. Kaushik S, Hord AH, Denson DD, McAllister DV, Smitra S, Allen MG, Prausnitz MR. Lack of pain associated with microfabricated microneedles. Anesth Analg 2001;92:502–504. [PubMed: 11159258]
25. Prausnitz MR. Overcoming skin's barrier: The search for effective and user-friendly drug delivery. Diabetes Technol Ther 2001;3:233–236. [PubMed: 11478330]
26. Lombry C, Dujardin N, Preat V. Transdermal delivery of macromolecules using skin electroporation. Pharm Res 2000;17:32–37. [PubMed: 10714605]
27. Jadoul A, Tanojo H, Preat V, Bouwstra JA, Spies F, Bodde HE. Electroperturbation of human stratum corneum fine structure by high voltage pulses: A freeze-fracture electron microscopy and differential thermal analysis study. J Invest Dermatol Symp Proc 1998;3:153–158.
28. Lee S, Kollias N, McAuliffe DJ, Flotte TJ, Doukas AG. Topical drug delivery in humans with a single photomechanical wave. Pharm Res 1999;16:1717–1721. [PubMed: 10571277]
29. Lee S, McAuliffe DJ, Flotte TJ, Kollias N, Doukas AG. Photomechanical transcutaneous delivery of macromolecules. J Invest Dermatol 1998;111:925–929. [PubMed: 9856797]
30. Menon GK, Kollias N, Doukas AG. Ultrastructural evidence of stratum corneum permeabilization induced by photomechanical waves. J Invest Dermatol 2003;121:104–109. [PubMed: 12839570]

31. Lee S, McAuliffe DJ, Mulholland SE, Doukas AG. Photomechanical transdermal delivery of insulin in vivo. Lasers Surg Med 2001;28:282–285. [PubMed: 11295766]
32. Upadhyay P. Enhanced transdermal-immunization with diptheria-toxoid using local hyperthermia. Vaccine 2006;24:5593–5598. [PubMed: 16735086]
33. Terahara T, Mitragotri S, Langer R. Porous resins as a cavitation enhancer for low-frequency sonophoresis. J Pharm Sci 2002;91:753–759. [PubMed: 11920760]
34. Tang H, Mitragotri S, Blankschtein D, Langer R. Theoretical description of transdermal transport of hydrophilic permeants: Application to low-frequency sonophoresis. J Pharm Sci 2001;90:545–568. [PubMed: 11288100]
35. Paliwal S, Menon GK, Mitragotri S. Low-frequency sonophoresis: Ultrastructural basis for stratum corneum permeability assessed using quantum dots. J Invest Dermatol 2006;126:1095–1101. [PubMed: 16528354]
36. Alvarez-Roman R, Merino G, Kalia YN, Naik A, Guy RH. Skin permeability enhancement by low frequency sonophoresis: Lipid extraction and transport pathways. J Pharm Sci 2003;92:1138–1146. [PubMed: 12761803]
37. Terahara T, Mitragotri S, Kost J, Langer R. Dependence of low-frequency sonophoresis on ultrasound parameters; distance of the horn and intensity. Int J Pharm 2002;235:35–42. [PubMed: 11879737]
38. Tachibana K. Transdermal delivery of insulin to alloxan-diabetic rabbits by ultrasound exposure. Pharm Res 1992;9:952–954. [PubMed: 1438012]
39. Joshi A, Raje J. Sonicated transdermal drug transport. J Control Release 2002;83:13–22. [PubMed: 12220834]
40. Turner NG, Ferry L, Price M, Cullander C, Guy RH. Iontophoresis of poly-L-lysines: The role of molecular weight? Pharm Res 1997;14:1322–1331. [PubMed: 9358543]
41. Grewal BS, Naik A, Irwin WJ, Gooris G, de Grauw CJ, Gerritsen HG, Bouwstra JA. Transdermal macromolecular delivery: Real-time visualization of iontophoretic and chemically enhanced transport using two-photon excitation microscopy. Pharm Res 2000;17:788–795. [PubMed: 10990196]
42. Turner NG, Guy RH. Iontophoretic transport pathways: Dependence on penetrant physicochemical properties. J Pharm Sci 1997;86:1385–1389. [PubMed: 9423151]
43. Turner NG, Guy RH. Visualization and quantitation of iontophoretic pathways using confocal microscopy. J Invest Dermatol Symp Proc 1998;3:136–142.
44. Wiechers JW, de Zeeuw RA. Transdermal drug delivery: Efficacy and potential applications of the penetration enhancer Azone. Drug Des Deliv 1990;6:87–100. [PubMed: 2080983]
45. Mitragotri S. Synergistic effect of enhancers for transdermal drug delivery. Pharm Res 2000;17:1354–1359. [PubMed: 11205727]
46. Lee PJ, Ahmad N, Langer R, Mitragotri S, Prasad Shastri V. Evaluation of chemical enhancers in the transdermal delivery of lidocaine. Int J Pharm 2006;308:33–39. [PubMed: 16321488]
47. Karande P, Jain A, Mitragotri S. Relationships between skin's electrical impedance and permeability in the presence of chemical enhancers. J Control Release 2006;110:307–313. [PubMed: 16313994]
48. Karande P, Jain A, Ergun K, Kispersky V, Mitragotri S. Design principles of chemical penetration enhancers for transdermal drug delivery. Proc Natl Acad Sci 2005;102:4688–4693. [PubMed: 15774584]
49. Afouna MI, Fincher TK, Zaghloul AA, Reddy IK. Effect of Azone upon the in vivo antiviral efficacy of cidofovir or acyclovir topical formulations in treatment/prevention of cutaneous HSV-1 infections and its correlation with skin target site free drug concentration in hairless mice. Int J Pharm 2003;253:159–168. [PubMed: 12593946]
50. Santoyo S, Ygartua P. Effect of skin pretreatment with fatty acids on percutaneous absorption and skin retention of piroxicam after its topical application. Eur J Pharm Biopharm 2000;50:245–250. [PubMed: 10962234]
51. Takahashi K, Sakano H, Numata N, Kuroda S, Mizuno N. Effect of fatty acid diesters on permeation of anti-inflammatory drugs through rat skin. Drug Dev Ind Pharm 2002;28:1285–1294. [PubMed: 12476874]
52. Kost J, Pliquett U, Mitragotri S, Yamamoto A, Langer R, Weaver J. Synergistic effect of electric field and ultrasound on transdermal transport. Pharm Res 1996;13:633–638. [PubMed: 8710759]

53. Tezel A, Sens A, Tuchscherer J, Mitragotri S. Synergistic effect of low-frequency ultrasound and surfactants on skin permeability. J Pharm Sci 2002;91:91–100. [PubMed: 11782900]
54. Le L, Kost J, Mitragotri S. Combined effect of low-frequency ultrasound and iontophoresis: Applications for transdermal heparin delivery. Pharm Res 2000;17:1151–1154. [PubMed: 11087051]
55. Scheuplein, R. Site variations in diffusion and permeability. In: Jarrett, A., editor. The physiology and pathophysiology of the skin. 1st edition. London: Academic Press; 1978. p. 1731-1752.
56. Fritsch WC, Stoughton RB. The effect of temperature and humidity on the penetration of C14 acetylsalicylic acid in excised human skin. J Invest Dermatol 1963;41:307–311. [PubMed: 14075455]
57. Zimmerer RE, Lawson KD, Calvert CJ. The effects of wearing diapers on skin. Pediatr Dermatol 1986;3:95–101. [PubMed: 3952034]
58. Roberts, MS.; Walker, M. Water, the most natural penetration enhancer. In: Walters, KA.; Hadgraft, J., editors. Pharmaceutical skin penetration enhancement. 1st edition. New York: Marcel Dekker; 1993. p. 1-30.
59. Bouwstra JA, Gooris GS, Salomons-de Vries MA, van der Spek JA, Bras W. Structure of human stratum corneum as a function of temperature and hydration: A wide-angle x-ray diffraction study. Int J Pharm 1992;84:205–216.
60. Bouwstra JA, Gooris GS, van der Spek JA, Bras W. Structural investigations of human stratum corneum by small-angle X-ray scattering. J Invest Dermatol 1991;97:1005–1012. [PubMed: 1748810]
61. Van Hal DA, Jeremiasse E, Junginger HE, Spies F, Bouwstra JA. Structure of fully hydrated human stratum corneum: A freeze-fracture electron microscopy study. J Invest Dermatol 1996;106:89–95. [PubMed: 8592088]
62. Warner RR, Stone KJ, Boissy YL. Hydration disrupts human stratum corneum ultrastructure. J Invest Dermatol 2003;120:275–284. [PubMed: 12542533]
63. Warner RR, Boissy YL, Lilly NA, Spears MJ, McKillop K, Marshall JL, Stone KJ. Water disrupts stratum corneum lipid lamellae: Damage is similar to surfactants. J Invest Dermatol 1999;113:960–966. [PubMed: 10594737]
64. Simon GA, Maibach HI. The pig as an experimental animal model of percutaneous permeation in man: Qualitative and quantitative observations—An overview. Skin Pharmacol Appl Skin Physiol 2000;13:229–234. [PubMed: 10940812]
65. Hammond SA, Tsonis C, Sellins K, Rushlow K, Scharton-Kersten T, Colditz I, Glenn GM. Transcutaneous immunization of domestic animals: Opportunities and challenges. Adv Drug Deliv Rev 2000;43:45–55. [PubMed: 10967220]
66. Galey WR, Lonsdale HK, Nacht S. The in vitro permeability of skin and buccal mucosa to selected drugs and tritiated water. J Invest Dermatol 1976;67:713–717. [PubMed: 1033956]
67. Gore AV, Liang AC, Chien YW. Comparative biomembrane permeation of tacrine using Yucatan minipigs and domestic pigs as the animal model. J Pharm Sci 1998;87:441–447. [PubMed: 9548896]
68. Reifenrath WG, Chellquist EM, Shipwash EA, Jederberg WW, Krueger GG. Percutaneous penetration in the hairless dog, weanling pig and grafted athymic nude mouse: Evaluation of models for predicting skin penetration in man. Br J Dermatol 1984;111:123–135. [PubMed: 6204672]
69. Bartek MJ, LaBudde JA, Maibach HI. Skin permeability in vivo: Comparison in rat, rabbit, pig and man. J Invest Dermatol 1972;58:114–123. [PubMed: 4622425]
70. Hallegot P, Minondo AM, Fiat F. Cryo-techniques applied to stratum corneum with description of a new sample holder for cryo-scanning electron microscopy of freeze-fractured samples. J Microscopy 1999;196:35–39.
71. Agarwal V, Singh M, McPherson G, John V, Bose A. Freeze fracture direct imaging of a viscous surfactant mesophase. Langmuir 2004;20:11–15. [PubMed: 15744989]
72. Jolly M, Swan AG. The effects on rat skin of prolonged exposure to water. Br J Dermatol 1980;103:387–395. [PubMed: 7437305]
73. Lindberg M, Forslind B. The effects of occlusion of the skin on the Langerhans' cell and the epidermal mononuclear cells. Acta Derm Venereol 1981;61:201–205. [PubMed: 6167101]

74. Lindberg M, Johannesson A, Forslind B. The effect of occlusive treatment on human skin: An electron microscopic study on epidermal morphology as affected by occlusion and dansyl chloride. Acta Derm Venereol 1982;62:1–5. [PubMed: 6175130]

75. Mikulowska A. Reactive changes in human epidermis following simple occlusion with water. Contact Dermatitis 1992;26:224–227. [PubMed: 1395558]

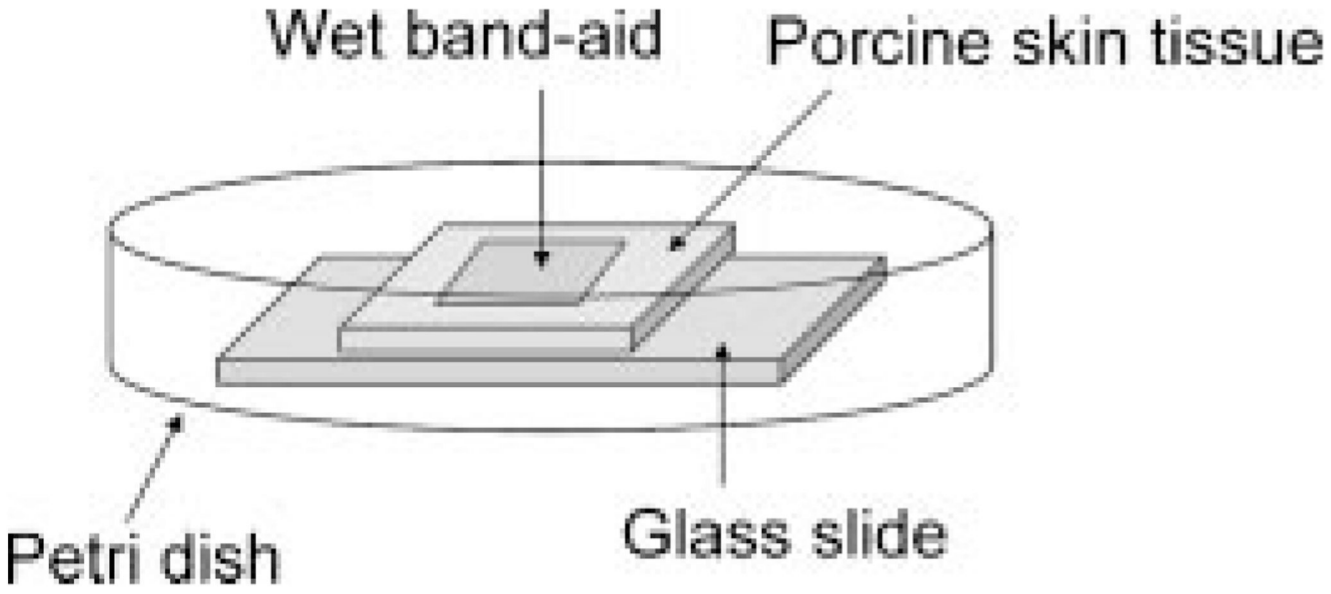

Figure 1.
Illustration of porcine skin hydrated using a wet band-aid.

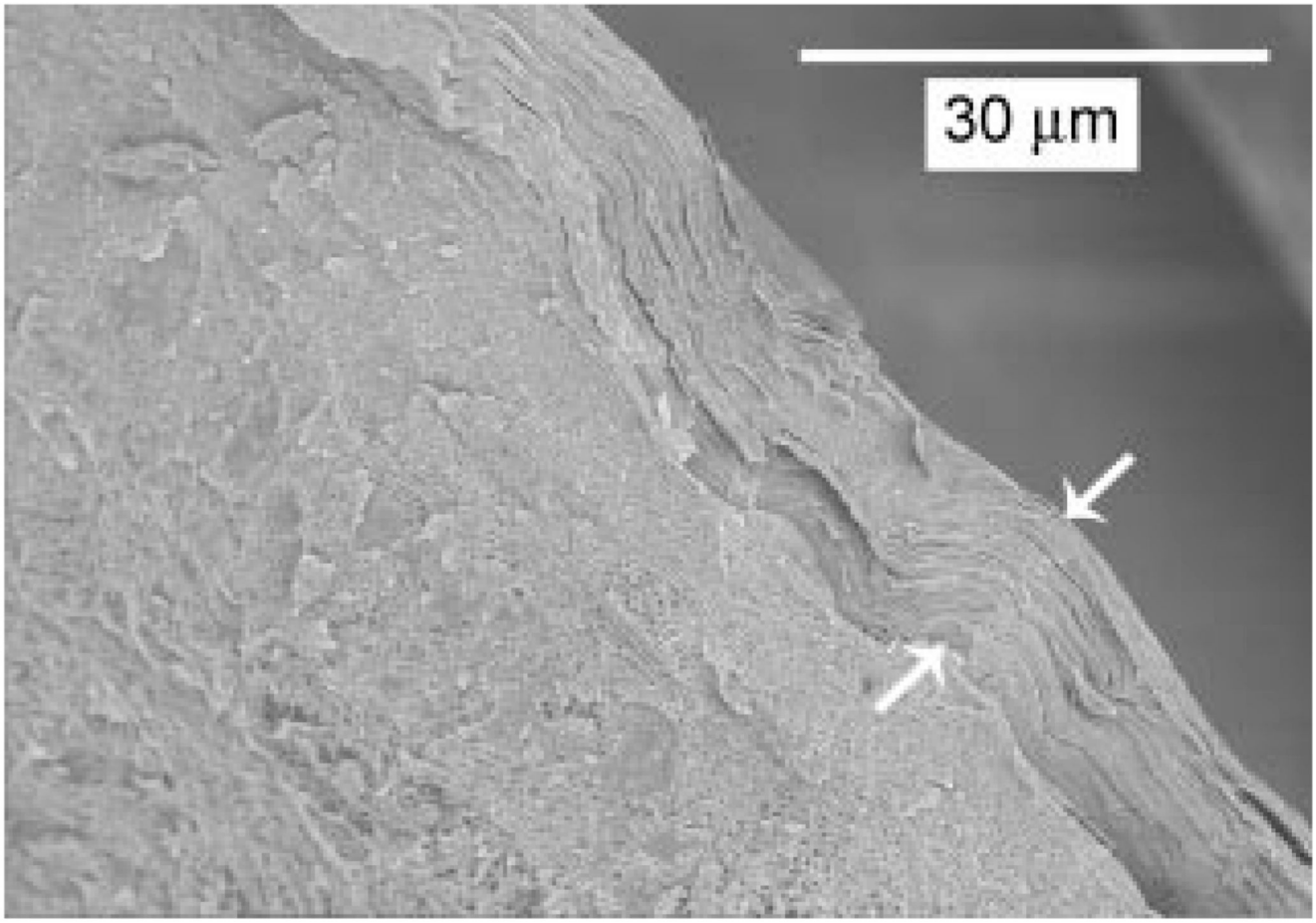

Figure 2.
Cryo-SEM image showing the cross-section of natively hydrated porcine skin obtained after cryo-fracturing. The stratum corneum, which runs diagonally from the top left to the bottom right in the picture, is seen overlying the viable epidermis. The stratum corneum of the untreated tissue is ~10 µm thick (marked by arrows) with a compact ultrastructure.

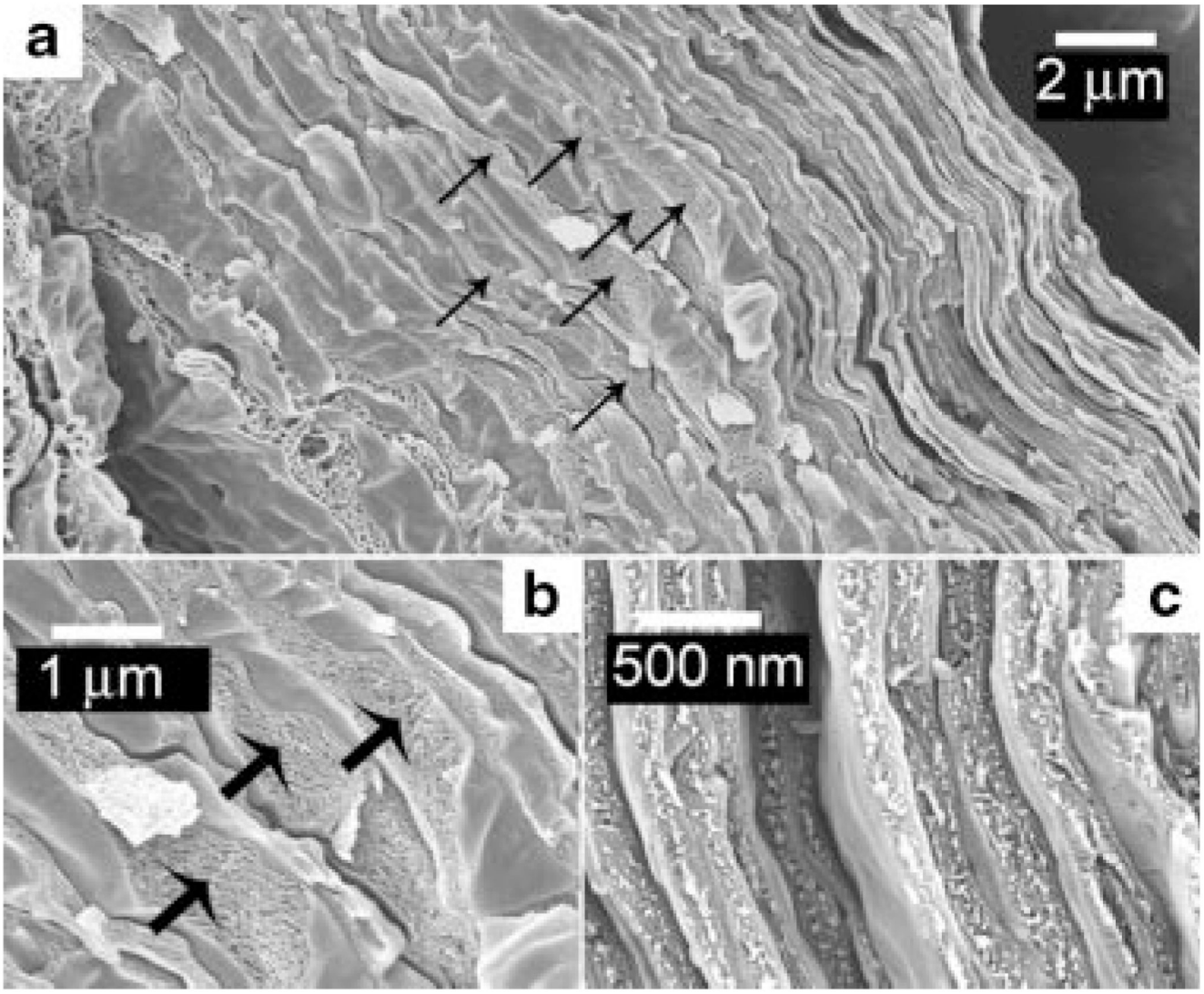

Figure 3.

Low and high magnification cryo-SEM images of the stratum corneum of natively hydrated porcine skin tissue. a: The stratum corneum consists of a dense outer layer and a less dense inner layer (each arrow marks the location of a corneocyte cell in the inner layer). b: The inner layers consist of irregular shaped corneocyte cells (indicated by arrows). Small gaps between corneocytes in b are artifacts of cryo-fracturing. c: The outer layer consists of densely packed flat sheets of corneocyte cells.

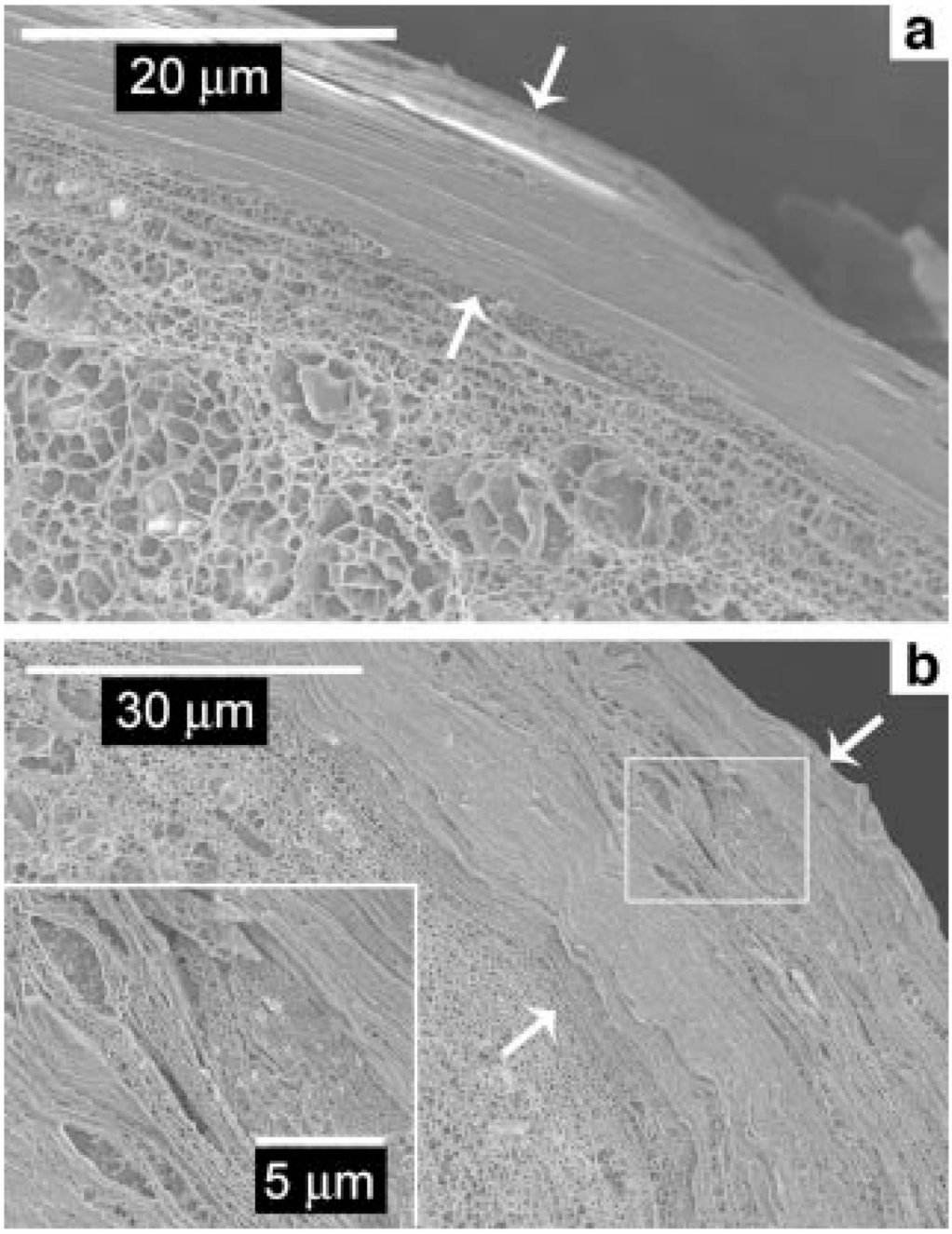

Figure 4.
a: Stratum corneum of porcine skin hydrated for an hour. b: Stratum corneum of highly hydrated porcine skin measuring slightly over 30 µm (marked by arrows). The inset, a high magnification image of the boxed region in (b) reveals separation of lipid bilayers to form water pools.

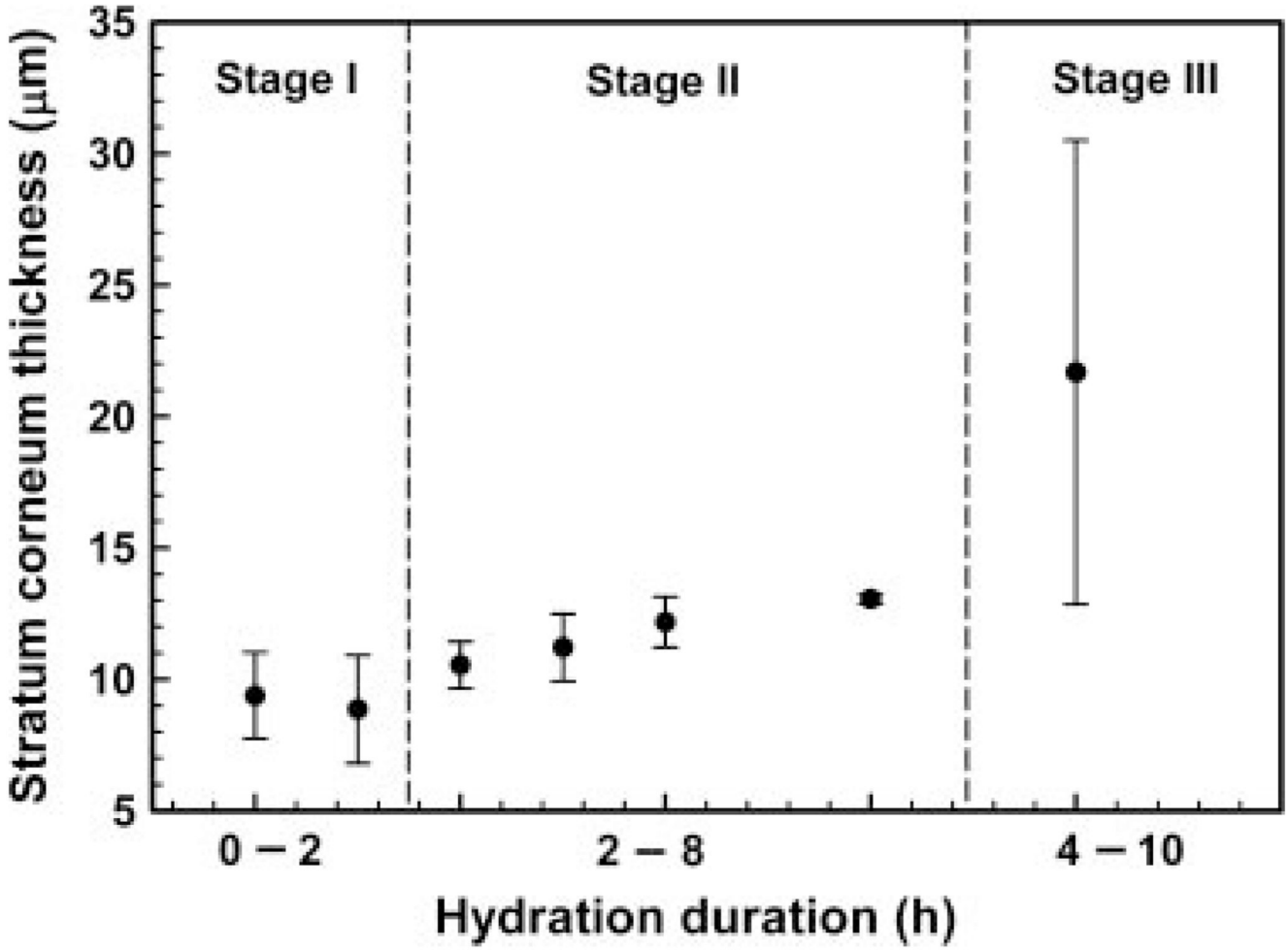

Figure 5.
Graph illustrating stratum corneum thickness at different hydration periods.

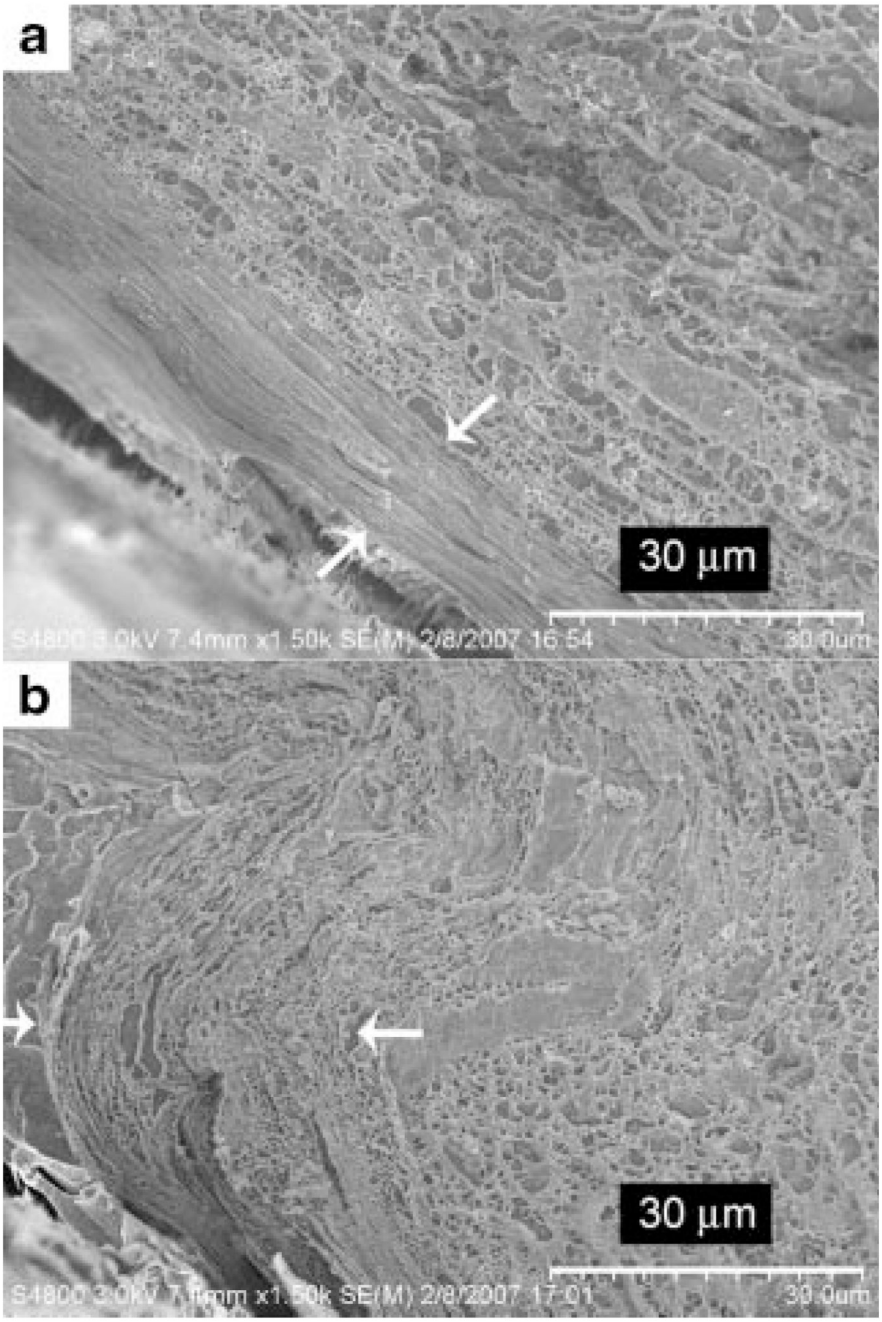

Figure 6.
Stratum corneum thickness of (a) nonruptured and (b) ruptured skin sections when hydrated for 8h (Stage III).

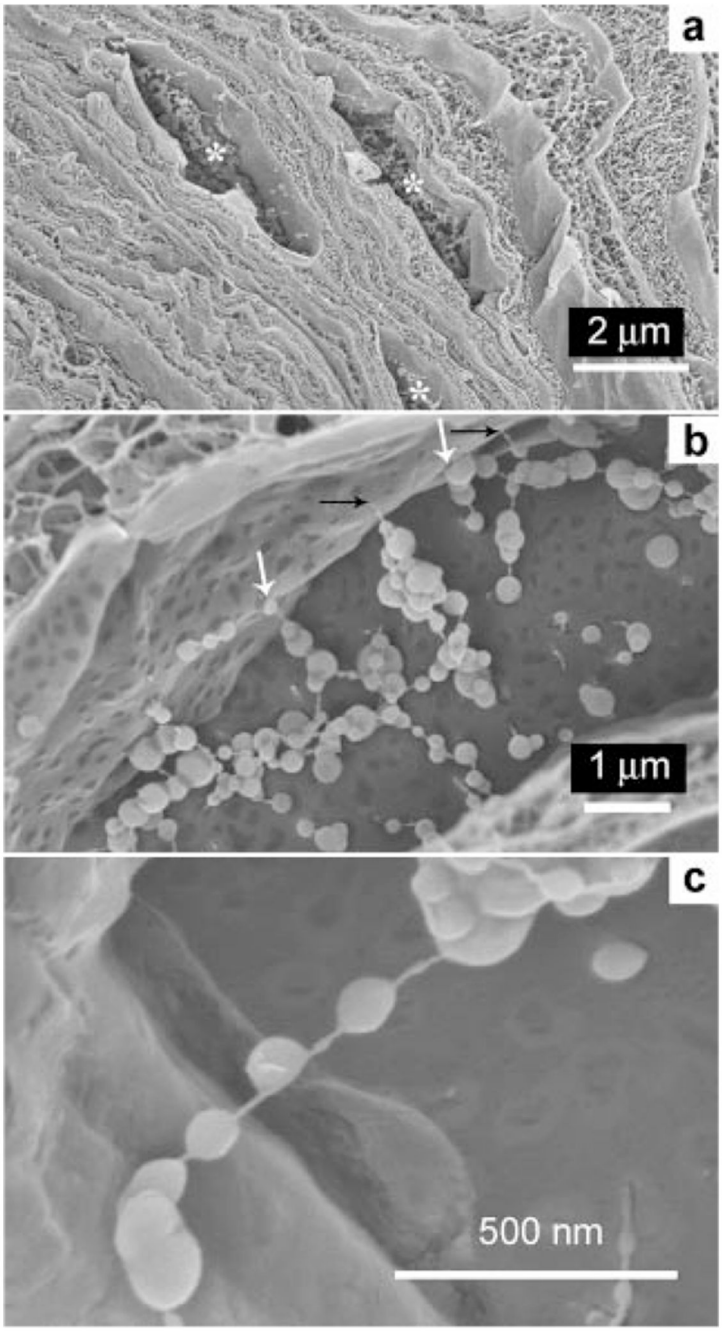

Figure 7.
Contents of cisternae in highly hydrated porcine skin. a: Cisternae (asterisks) frequently contain particulate matter. b: Agglomerated polydisperse spheres (or beads) attached through thin strings to form networks in a cisternae. Some beads are fused to the cisternal walls (white arrows), others attach to the cisternal walls through thin strings (black arrows). The beads may be disrupted lipids that have rearranged and formed multilamellar vesicles. c: High magnification image of globular structures in a cisternae.

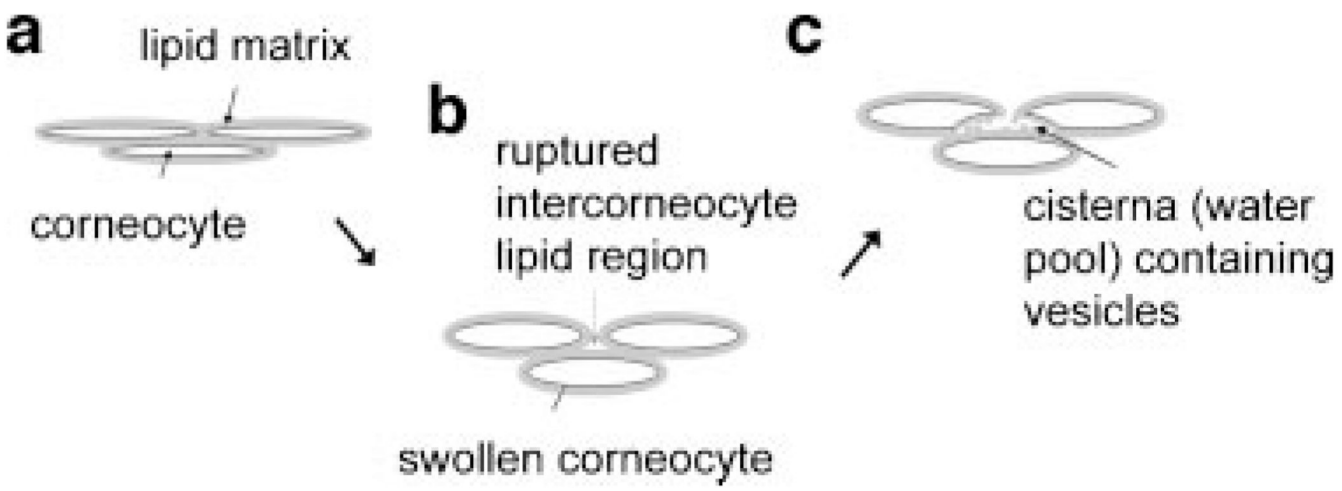

Figure 8.
Illustration depicting changes in corneocytes and the intercellular lipid matrix upon prolonged external hydration. a: Initially, corneocytes are densely packed in the stratum corneum. b: Upon external hydration, corneocytes become swollen leading to small ruptures in the intercellular lipid matrix. c: The ingress of water leads to the formation of a cisterna containing spherical lipid aggregates.

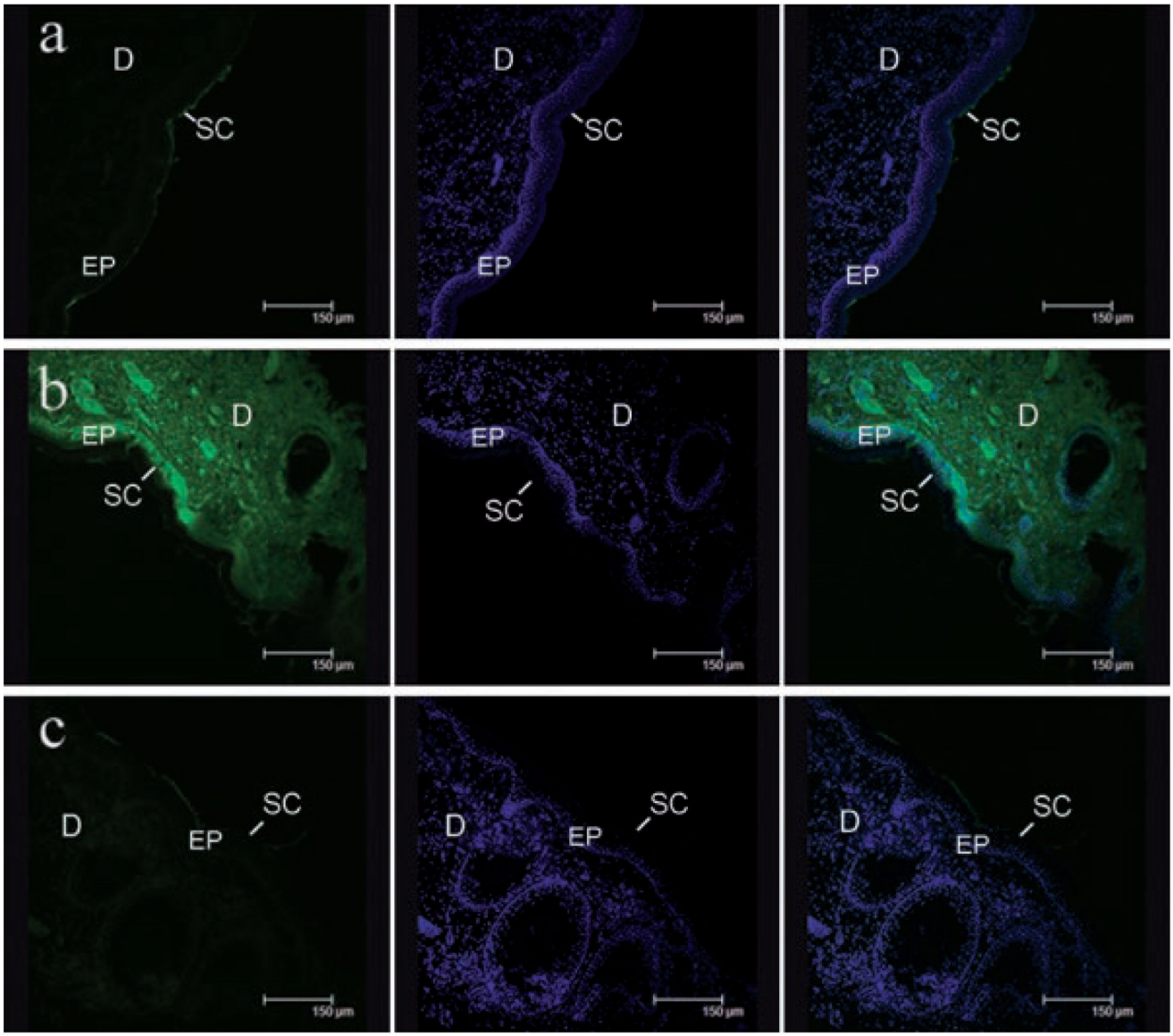

Figure 9.

Confocal images of (a) natively hydrated, (b) highly hydrated, and (c) restored porcine skin tissue after FITC-BSA was loaded for an hour. The three vertical columns shows images of skin tissue obtained through the FITC channel (left), the DAPI channel (middle), and an overlay of FITC and DAPI channels (right). The green color indicates presence of FITC-BSA while the blue color shows the DAPI-stained cell nuclei. Scale bar = 150 μm. SC, stratum corneum; EP, epidermis; D, dermis.

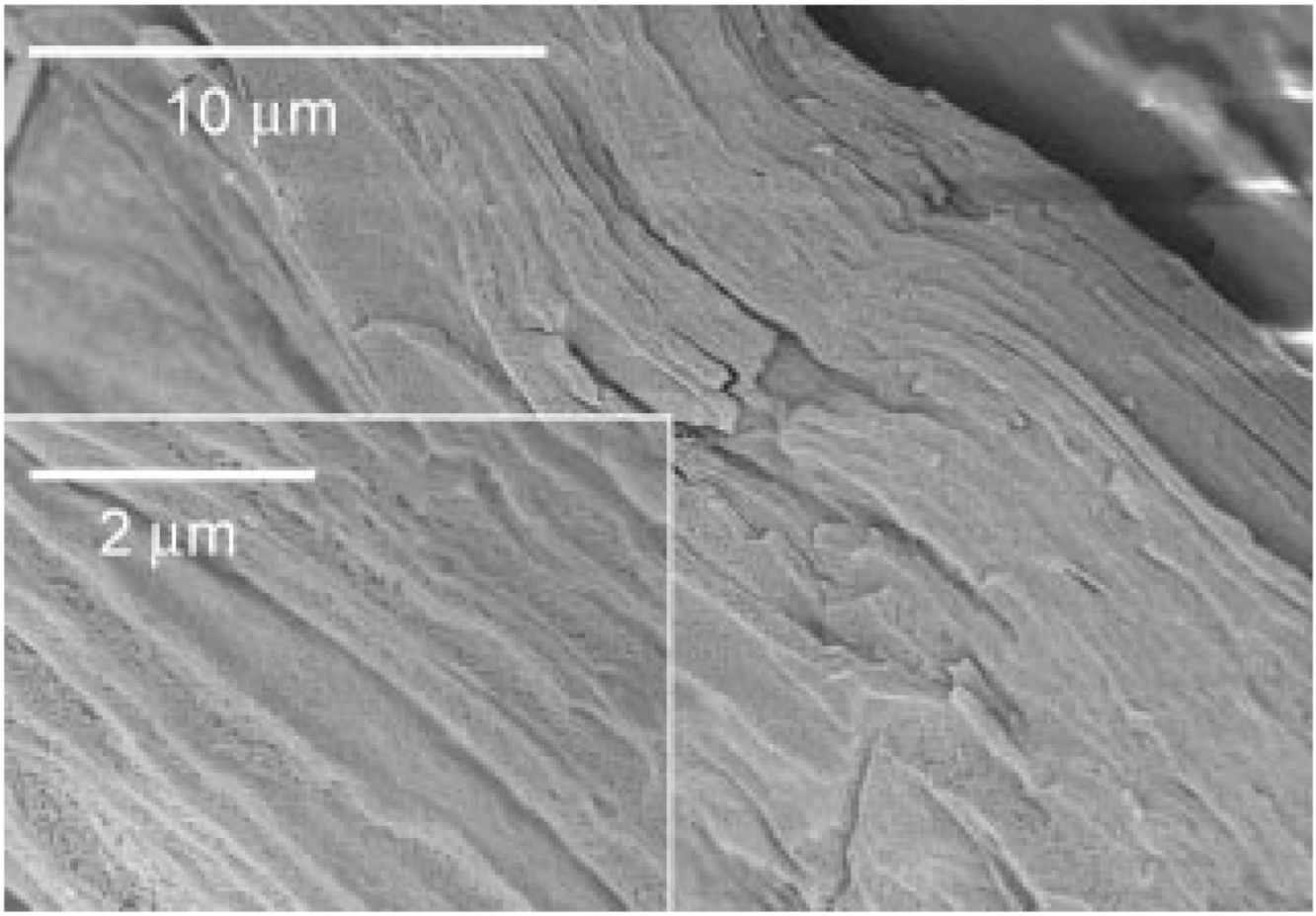

Figure 10.
Restored porcine skin tissue shows absence of huge cisternae and a compact ultrastructure. Inset shows a higher magnification image of the corneocytes in restored skin.